165, 191-198.

52) Tsukigawa, K., Nakamura, H., Fang, J., Otagiri, M. and Maeda, H. (in preparation/press) Effect of depegylation at the tumor site on intracellular uptake and therapeutic effect of pegylated zinc protoporphyrin (PEG-ZnPP).

53) Saisyo, A., Nakamura, H. and Maeda, H. (2012) Synthesis and characterization of SMA-copolymer-Cisplatin complex for tumor targeted delivery based on the EPR-effect. Abstract No. 3081, 71st Annual Meeting of the Japanese Cancer Association, Sept. 19-21, Sapporo, p. 326.

54) Kunimoto, S., Miura, K., Takahashi, Y., Takeuchi, T. and Umezawa, H. (1983) Rapid uptake by cultured tumor cells and intracellular behavior of 4'-*O*-tetrahydropyranyladriamycin. J. Antibiot (Tokyo) **36**, 312-317.

55) Gomer, C.J. and Ferrario, A. (1990) Tissue distribution and photosensitizing properties of mono-L-aspartyl chlorin e6 in a mouse tumor model. Cancer Res. **50**, 3985-3990.

56) Fang, J., Sawa, T., Akaike, T., Akuta, T., Greish, K.. Hamada A. and Maeda, H. (2003) *In vivo* antitumor activity of pegylated zinc protoporphyrin: Targeted inhibition of heme oxygenase in solid tumor. Cancer Res. **63**, 3567-3574.

57) Fang, J., Akaike, T. and Maeda, H. (2004) Antiapoptotic role of heme oxygenase and its potential as an anticancer target. Apoptosis **9**, 27-35.

58) Mayerhofer, M., Florian, S., Krauth, M.T., Aichberger, K.J., Bilban, M., Marculescu, R., Printz, D., Fritsch, G., Wagner, O., Selzer, E., Sperr, W.R., Valent, P. and Sillaber, C. (2004) Identification of heme oxygenase-1 as a novel BCR/ABL-dependent survival factor in chronic myeloid leukemia. Cancer Res. **64**, 3148-3154.

59) Herrmann, H., Kneidinger, M., Cerny-Reiterer, S., Rülicke, T., Willmann, M., Gleixner, K.V., Blatt, K., Hörmann, G., Peter, B., Samorapoompichit, P., Pickl, W., Bharate, G.Y., Mayerhofer, M., Sperr, W.R., Maeda, H. and Valent, P. (2012) The Hsp32 inhibitors SMA-ZnPP and PEG-ZnPP exert major growth-inhibitory effects on CD34^{+}/CD38^{+} and CD34^{+}/CD38^{-} AML progenitor cells. Curr. Cancer Drug Targets **12**, 51-63.

Figure Legends

Fig. 1.   Hypothetical plasma profile of low-MW free drugs (a) (*e.g.*, DOX or pirarubicin) and their polymer conjugates (b-d). The drug concentration in plasma after i.v. injection of low-MW (parent) drugs (a) decreased rapidly. Representative polymer conjugate micelles and the liposome complex remained in the plasma at high levels (b-e). Although (b) is the block copolymer micellar drug of DOX burst rapidly, with a 50% decrease in 1 hour after i.v. administration. No therapeutic benefit from the EPR effect was thus seen, because of the poor stability of the micelle. (c) A styrene-co-maleic acid (SMA)-polymer DOX conjugate. (d) An SMA-polymer tetrahydropyranyl doxorubicin (THP) conjugate. For a stable liposome complex such as the one with Doxil® (e), the liposomal drug concentration in plasma continued at a high level. This liposome complex of a pegylated stealth liposome of DOX was too stable, however, with little drug release and thus little therapeutic effect.   The conjugate in (d) demonstrated a more favorable result than did that in (b), (c) or (e).

Fig. 2.   *In vivo* fluorescence imaging of tumors selectivity based on EPR effect via a fluorescent nanoprobe. Polymer-conjugate fluoroprobe used here is polymer-N-(2-hydroxypropyl)methacrylamide (HPMA) conjugated with zinc protoporphyrin (ZnPP) (MW~50 kDa). Whole-body fluorescence of S180 tumor-bearing mice. (A) After injection with HPMA-ZnPP, fluorescence imaging revealed tumor-selective drug accumulation. (B) Injection of low-MW free ZnPP (MW~770 Da) showed no tumor-selective drug accumulation and no fluorescence. (A') Normal light

view of A. Images were obtained with an IVIS XR *in vivo* fluorescence detector (Caliper

Life Science, Hopkinton, MA) 48 hours after i.v. injection of each drug (both at 15 mg/kg

ZnPP equivalent). Modified from Ref. 30 and reproduced with permission.

Fig. 3. (A) Theoretical mechanism of NO generation and increase in drug delivery by use

of NG (nitroglycerin). NO is generated from nitrite, predominantly in hypoxic tumor

tissues rather than normal tissues. (B) NG enhanced blood flow in tumor tissue but not

in normal tissue (thigh muscle). Blood flow was measured with a laser flowmeter

(ALF-21; Advance Co., Ltd., Tokyo, Japan). S-180 tumor-bearing mice with tumor

diameters of 6–7 mm were anesthetized and placed on a warm pad (30–35℃). The blood

flow was monitored at first for 5 minutes to confirm that it was stable, and then NG at

dose of 1.0 mg/mouse was applied to the dorsal skin. Blood flow in the thigh muscle was

measured after application of NG at a dose of 1.0 mg over the skin anywhere. Error bars

show 95% confidence intervals. The concentration of NG was 20 mg/g ointment

(Vaseline). Differences between muscle and tumor were compared with two-sided

Wilcoxon tests.   (C) Delivery of the putative macromolecular drug Evans blue-albumin

(70 kDa) to tumor tissue, which increased 2-3-fold after NG application. (D) Dose

response to NG and delivery to different murine tumors (Meth-A, C38). Modified from

Ref. 48. Reproduced with permission from [38].

Fig. 4.   (A) Metastatic tumor in the lung and the EPR effect.   Colon 26 tumor (5×10^6

cells) was implanted on the dorsal skin of a BALB/c mouse, and after about 3 months

the lung was removed and examined macroscopically, 24 hours after i.v. injection of

Evans blue dye.   Blue nodules (arrows) demonstrate that metastatic tumors exhibited

the EPR effect, with selective tumor uptake of dye.   (B) In this model, after i.v. injection

of 30 mg/kg polymer-conjugated pirarubicin (P-THP), all tumor nodules disappeared,

and all six mice in this group survived at 90 days in good health. In contrast, free

low-MW pirarubicin at about the maximum tolerable dose of 5 mg showed little

therapeutic effect (middle).

Fig. 5.   Chemical structures of THP conjugated to different polymers and their

pharmacological and antitumor effect.   (A) is the HPMA polymer conjugated THP, and

(B) is the SMA-copolymer conjugated THP. Toxicity was assessed by analysis of body

weight (C). Tumor and tissue distribution is shown in (D) and antitumor effect by tumor

volume in (E).   In contrast to free THP, P-THP (HPMA-THP) had no toxicity up to 100

mg/kg.   Free THP at 7 mg/kg, the LD_{50}, did not eradicate tumors.   At 15 mg/kg, P-THP

completely suppressed the tumors. P-THP was tolerated at doses >60 mg/kg (not shown)

(from Ref. 41, reproduced with permission).

Fig. 6.   Chemical structure of polymer HPMA(P)-conjugated ZnPP IX: polymer-zinc

protoporphyrin conjugate. From Ref. 51. Reprinted with permission, Elsevier Science.

Fig. 7. Autochthonous breast cancer in rats induced by DMBA treatment. (A) Tumor

image under normal light (top), and fluorescence image (IVIS, fluorescence imaging

system) (below). (B) Therapeutic effect of HPMA polymer zinc protoporphyrin (P-ZnPP)

conjugate administered once at 20 mg/kg i.v., after which endoscopic light was applied

at 0% or 40% power output for 5 minutes (×2). (C) Views of *in vivo* breast tumor treated

with PDT on the right, with the control group (no treatment) on the left. Therapeutic protocols are the same as those in (B). A significant size reduction on day 30 and complete eradication on day 50 are obvious.

Table 1. Factors and mediators involved in the EPR effect in cancer and inflammation, and their responsible enzymes or effectors[a].

EPR effect-enhancing factors/mediators	Enzymes responsible for factors	Comments, actions of enzymes and factors, or sources of factors
1. Bradykinin (kinin)	Kallikrein and other proteases, plasminogen activator produce bradykinin	Angiotensin I-converting enzyme (ACE) degrades kinin; ACE-inhibitor potentiates activity by blocking kinin degradation. Kinin induces NO synthase
2. Nitric oxide (NO)	Nitric oxide synthase (NOS), inducible isoform of NOS (iNOS)	Nitroglycerin, isosorbide dinitrate (ISDN, Nitrol®), and nitroprusside yield nitrate, and nitrite-reductase, which occurs in hypoxic tissue (tumor), generates NO in hypoxic tumors.
3. Prostaglandins (PGs)	Cyclooxygenase 2 (COX-2)	PGI_2 agonist/beraprost affect the EPR effect
4. Carbon monoxide (CO)	Heme oxygenase-1 (HO-1)	Hemin, NO, and ultraviolet light and heat induce induce HO-1
5. Peroxynitrite ($ONOO^-$)	Generated by NO + $O_2{}^{\cdot-}$	Extremely rapid reaction. Activate MMP/collagenase
6. Matrix metalloproteinase (MMP), or collagenase ($\leftarrow$ proMMP)[b]	Procollagenase activation by $ONOO^-$	$ONOO^-$ activates pro-MMP[b] $\rightarrow$ MMP
7. Vascular endothelial growth factor (VEGF/VPF)	Nitric oxide synthase (NOS)	NO, endotoxin, and other cytokines can induce this VEGF
8. Tumor necrosis factor α (TNF-α) and TFG-ß inhibitor	Cytokines, growth factor	Induces inflammation and normalization of tumor vasculature
9. Heat	Heat shock protein, HO-1 (HSP-32)	e.g. HO-1 and inflammation etc.

See text for detail.

[a]Above factors are most common mediators of inflammation and cancer that facilitate extravasation.
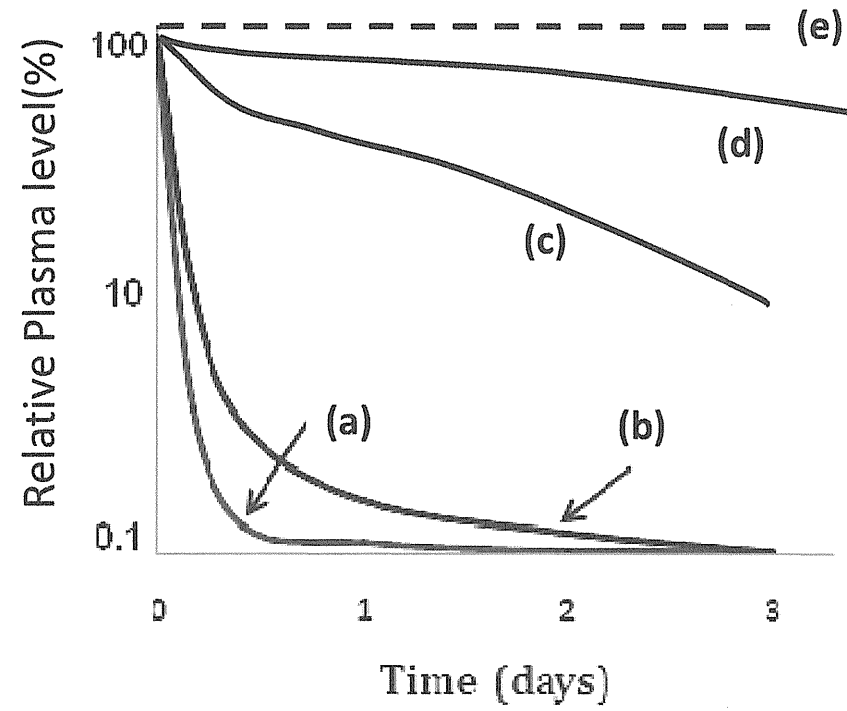
[b]proMMP: pro-matrix metalloproteinase (collagenase) is activated by $ONOO^-$ or by other proteases.   See text for detail.

Table 2. Strategies to overcome the heterogeneity of the EPR effect, and augmentation of the EPR effect to enhance tumor drug delivery.[a]
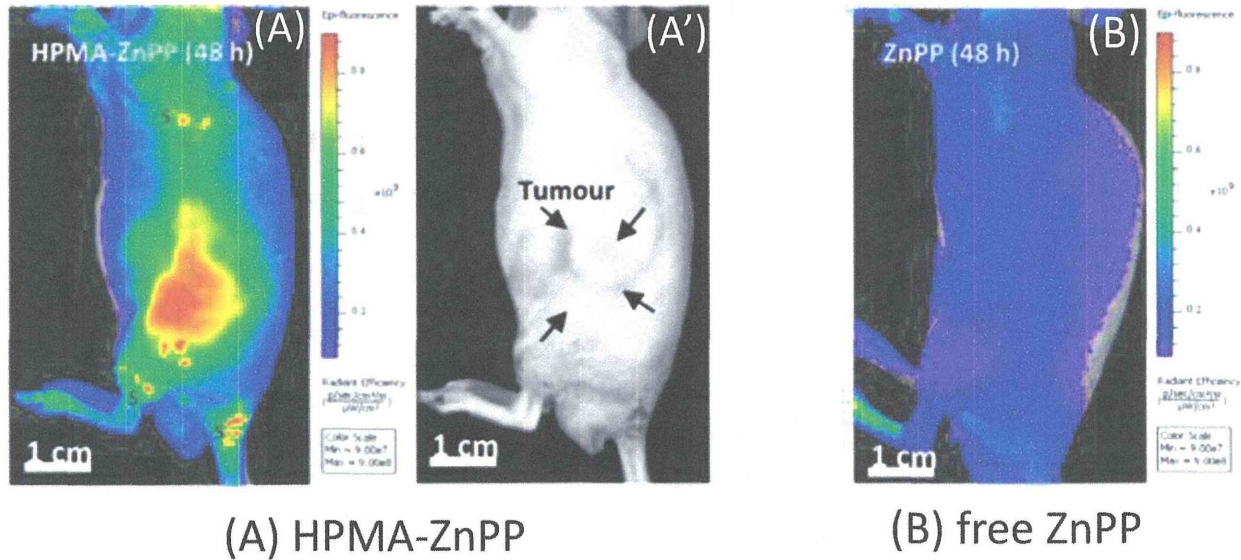
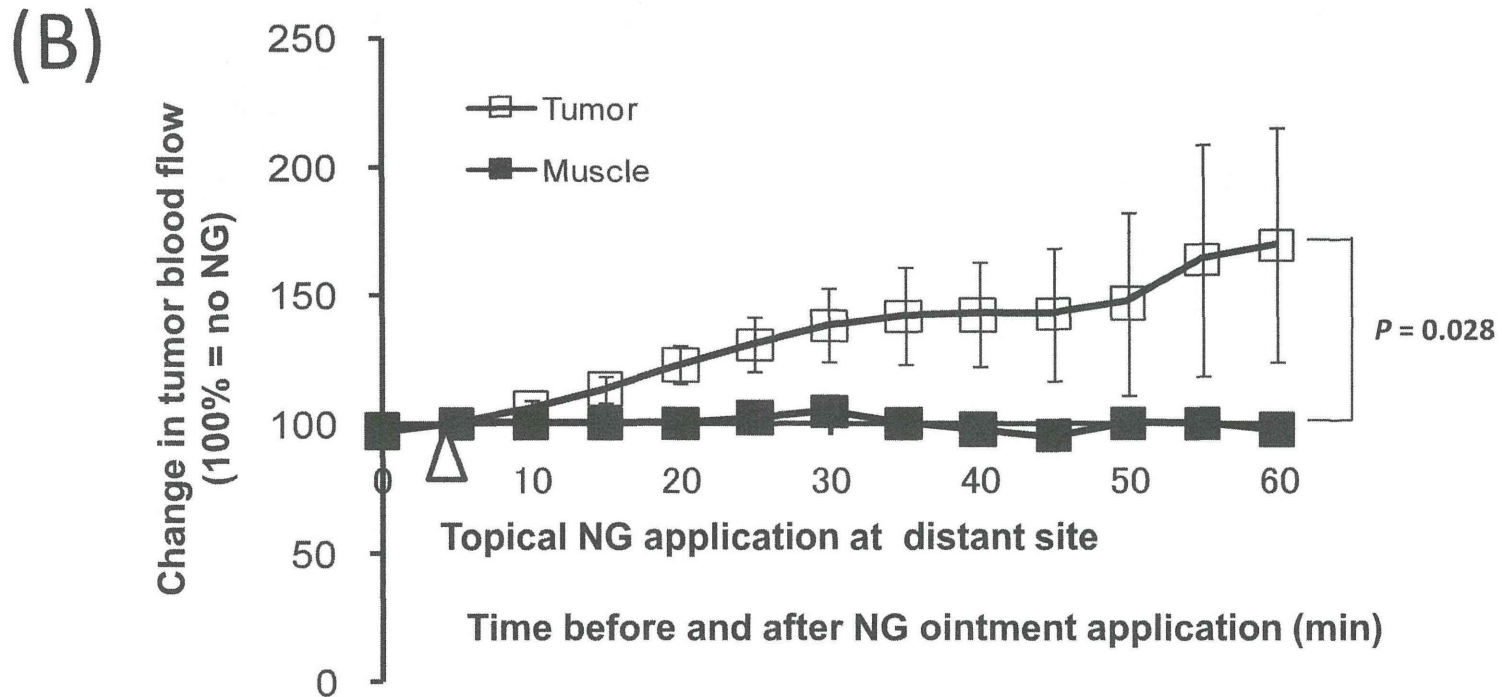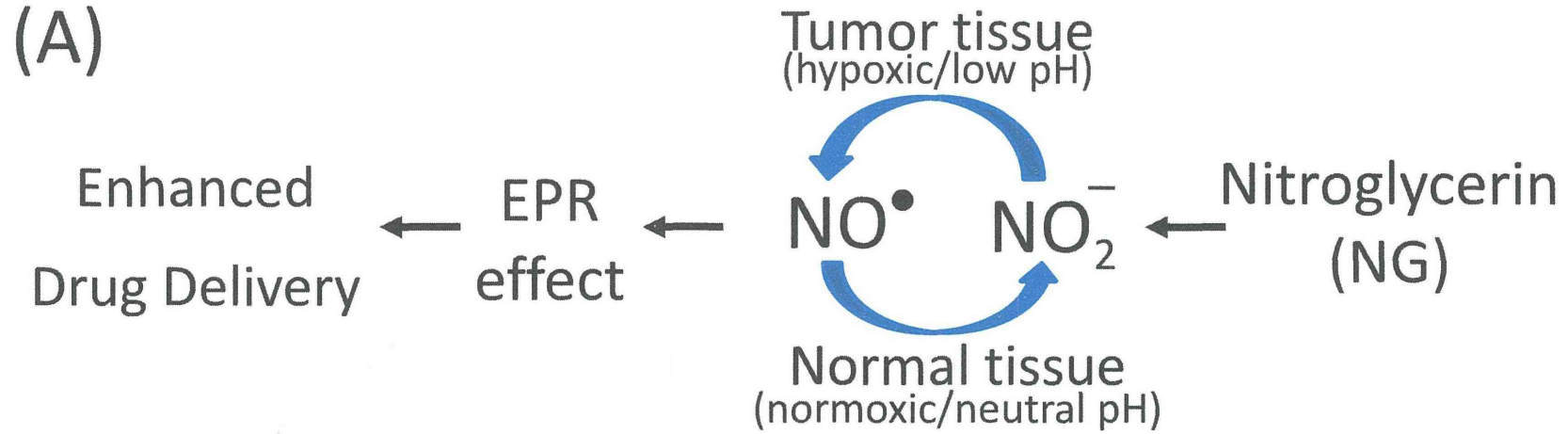| Methods[a]	Mechanism	Remarks
1. Use of angiotensin II-induced hypertension	Hydrodynamic; vasoconstriction induced hypertension → mechanical opening of endothelial cell-cell gaps passively at tumor.	Drug is infused into the tumor-feeding artery via catheter. EPR can be enhanced.
2. Use of angiotensin I-converting enzyme (ACE) inhibitor such as enalapril	Selectively elevates the kinin level only in tumors, by inhibiting kinin degradation by ACE-inhibitor, which occurs in the tumor tissue.	Given orally, very safe, clinically proven. EPR enhancer.
3. Use of nitroglycerin given topically by dermal patch, or by infusion via the tumor-feeding artery	Generates NO in hypoxic tumor issue selectively. See analogy to angina pectoris.	Nitroglycerin, isosorbide dinitrate (ISDN, Nitrol®), nitroprusside, and others; clinically proven (see text). EPR enhancer.
4. Use of prostaglandin (PG) I_2 analogue, beraprost sodium	PG agonist effect (with the $t_{1/2}$ more than 100 times longer in plasma than PGI_2) when given orally.	EPR enhancer.
5. Use of TGF-β-inhibitor	TGF-β is tumor growth and differentiation factor. Facilitate productive of extracellular matrix. The inhibitor counteracts to restore vascular maturation and normalization, which may be affected by vascular mediator.	Shown effective in the pancreatic cancer in vivo model.
6. Use of induction of HO-1, or a CO generator (ruthenium tricarbonyl, CORM2[b])	Zn protoporphyrin or hemin-polymer conjugates induce HO-1 in tumors; use of CORM2 generates CO. See text.	No data available for in vivo therapeutic efficacy.

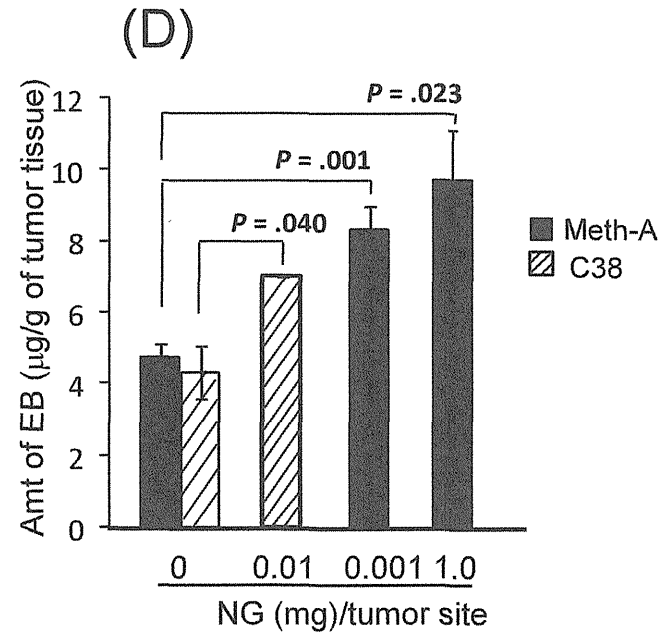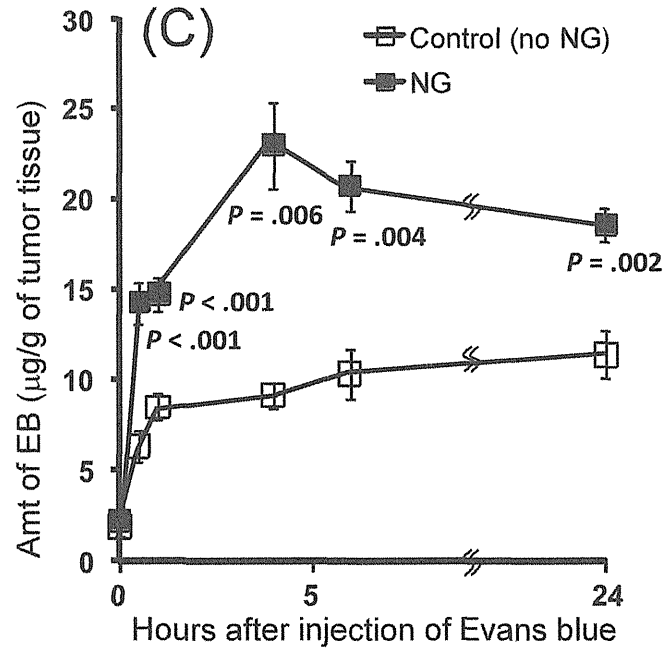[a]These strategies will be effective only with nanoparticle or polymeric drugs.

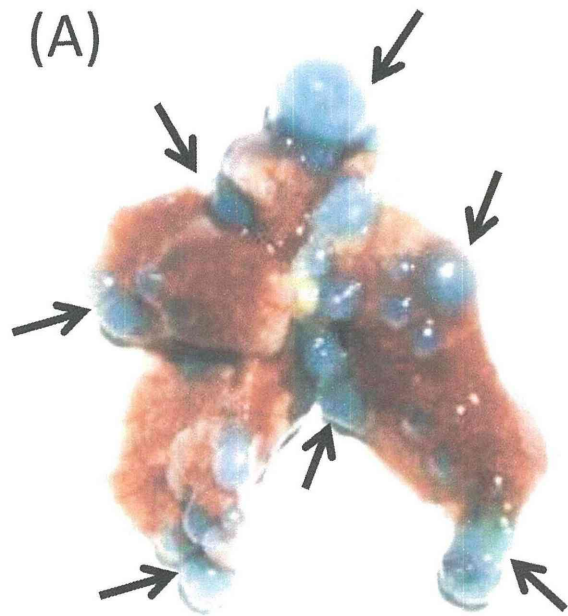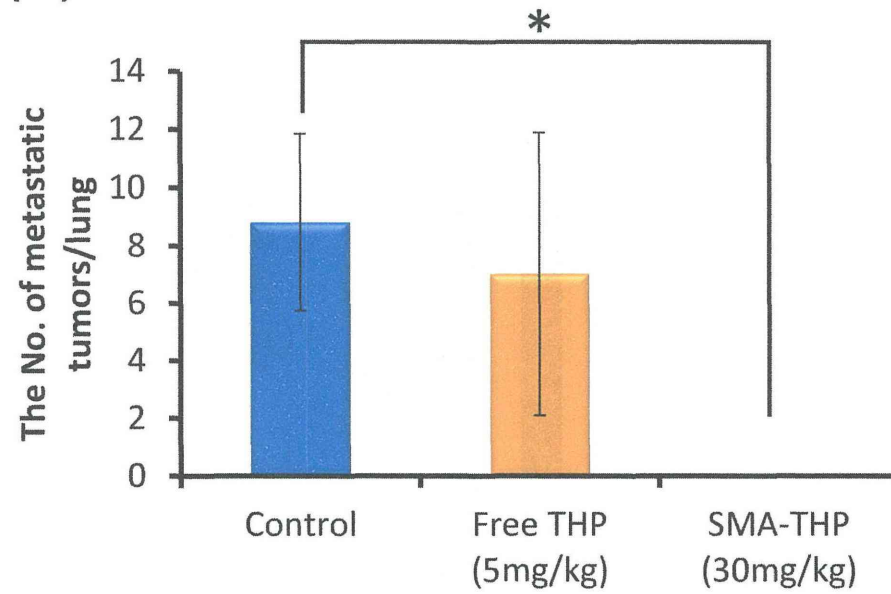[b] *Carbon monoxide* releasing molecule, derivative of ruthenium oxide.

Figure 4

Figure 2

(A) HPMA-ZnPP   (B) free ZnPP

(A)

Tumor tissue
(hypoxic/low pH)

Enhanced Drug Delivery ← EPR effect ← $NO^{\bullet}$ ⇄ NO_2^- ← Nitroglycerin (NG)

Normal tissue
(normoxic/neutral pH)

(B)

Change in tumor blood flow (100% = no NG)

— Tumor
— Muscle

$P = 0.028$

Topical NG application at distant site

Time before and after NG ointment application (min)

(A)

(B) Effect on metastatic lung cancer

Figure 5

(A)

(B)

(C)

15 mg/kg

No treatment

PHPMA-hyd-THP

Free-THP

Body weight (g)

Days after tumor inoculation

(D)

A. Parental free THP

Non-conjugated free THP

Arbitrary fluorescence intensity

B. HPMApolymer-THP

■ Tumor
⊔ Heart
⊠ Kidney
⊟ Spleen
⊿ Lung
⊠ Intestine
■ Liver
⊞ Plasma

5 h   24 h   48 h   72 h

(E)

15 mg/kg

No treatment

Free-THP

PHPMA-hyd-THP

Tumor volume (mm³)

Days after tumor inoculation

(A) Bright view of tumor. Fluorescent view of tumor. DMBA induced autochthonous breast cancer in rat.

(B) DMBA induced rat breast cancer model (autochthonous/orthotopic tumors) in rats. Tumor Volume (mm3) vs Days after treatment. Control; Drug (20mg/kg); Drug (20mg/kg) + Light (40%).

(C) Control; HPMA-ZnPP+Light. 0day, 30day, 60day.
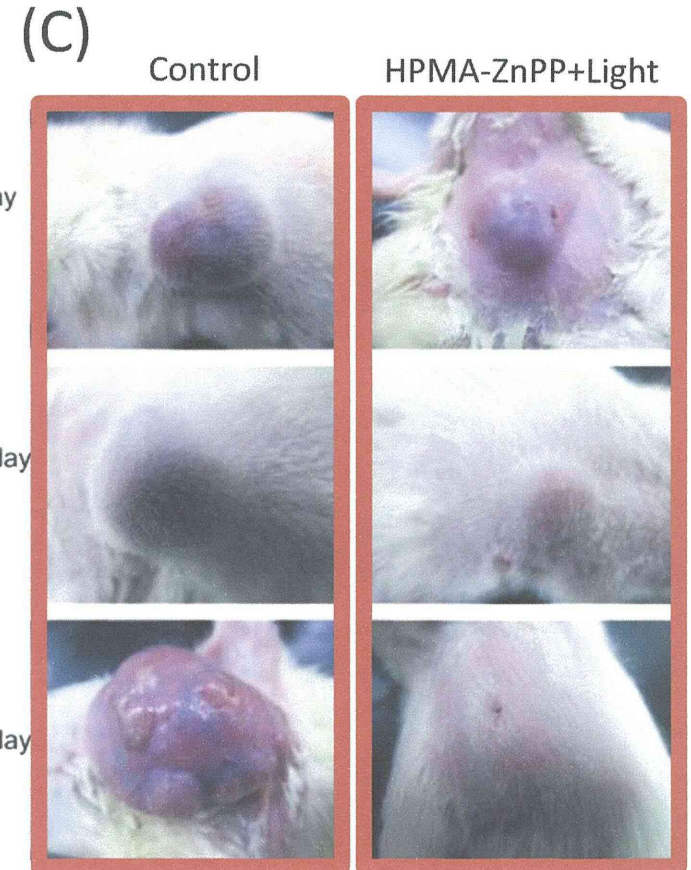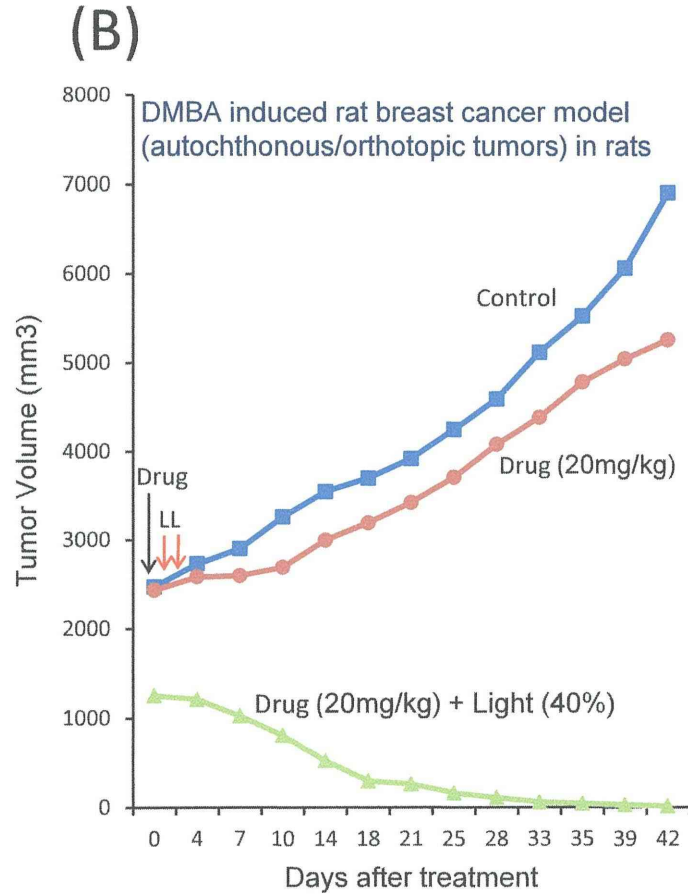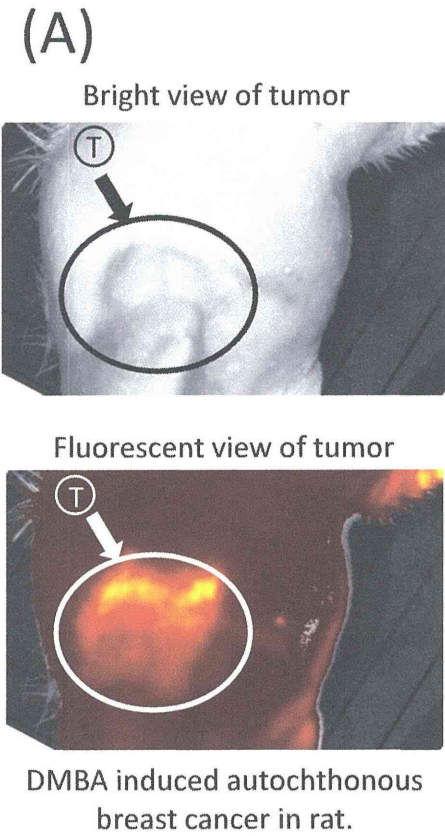
Research Spotlight / News and Analysis

Emergence of EPR Effect Theory and Development of Clinical Applications for Cancer

Therapy

Hiroshi Maeda

Institute of Drug Delivery Science, Sojo University, Kumamoto, Japan

Historical background of the enhanced permeability and retention (EPR)

effect

This is a personal recollection of how we discovered the EPR effect for tumor

selective delivery of anticancer drugs. The story of the EPR effect has three

components: (i) development of the macromolecular drug (poly(maleic

acid-styrene)-conjugated neocarzinostatin, or SMANCS), (ii) studies of infection and

inflammation and the vascular permeability mediator bradykinin (BK), and (iii) biology

and pharmacology of cancer. The first component involved synthesis of macromolecular

drugs (now called nanomedicines), because drugs of low molecular weight (MW) demonstrated no EPR effect. In 1960s, we isolated antitumor protein neocarzinostatin (NCS, MW 12 kDa) from culture filtrates of *Streptomyces carzinostaticus*, and determined its characteristics, chemistry (structure), and pharmacology (1). At that time, very little was known about the pharmacology of protein drugs. These studies were the beginning of development of the polymer drug SMANCS (1).

Vascular permeability in infection and inflammation

The second component of this endeavor was related to bacterial infection: the pathogenic effect of bacterial proteases, which infecting bacteria produce. These investigations led to the discovery of the activation of the proteolytic cascade that resulted in generation of BK, which is the most potent pain-inducing endogenous peptide and facilitates extravasation of macromolecules or plasma proteins at infection sites (2). This extravasation in inflamed tissues is a common phenomenon also observed in viral (e.g., influenza virus) infections that cause pneumonia and inflammation. Our most intriguing finding was simultaneous generation of superoxide (anion) radical ($O_2{}^{\bullet-}$) and nitric oxide (NO) (via activation of nitric oxide synthase) (3,4). This *in vivo* reaction produced a potent tissue-damaging peroxide ($ONOO^-$) that also

2

activates collagenases (e.g., metalloproteinase-2) and other enzymes, which enhance

vascular permeability. Just as for bacterial protease, the BK-generating cascade

occurred in cancer tissues (5,6); formation of pleural and ascetic fluids in

carcinomatosis also depends on generation of BK and other vascular mediators.

Another project at my department at Kumamoto University Medical School

concerned cancer chemotherapy—the third component leading to discovery of the EPR

effect.   We investigated the accumulation of SMANCS in tumors after intravenous

injection.   To our surprise, its accumulation in tumors was more marked than

accumulation in other normal tissues or organs (1,6-8).   We therefore studied the

accumulation of the most biocompatible macromolecules (e.g. albumin) in a

tumor-bearing mice.   Most interestingly, albumin accumulation in tumors increased

progressively with time, for more than a few days (8), and its concentration in tumors

was higher than its concentration in plasma at several hours after intravenous injection

(1,6-8). In contrast to these macromolecules, low-MW compounds (e.g., doxorubicin)

disappeared within a few hours. Uptake of macromolecules by normal tissues such as

the kidney, liver, muscles, and intestine was far lower (1/10-1/30) than uptake by tumors,

and the macromolecules were gradually cleared from normal tissues (via lymphatics) in

a week, whereas their tumor concentration remained quite high for weeks or longer

3

(4,8,9). This retention was a unique feature of tumor tissue, so the word *retention* was incorporated into the term EPR effect. We continued investigating this phenomenon, in collaboration with Professors Ruth Duncan of the Univ. of Birmingham, UK and Karel Ulbrich of Inst. of Macromolecular Chemistry, Prague, Czech Republic, by using highly biocompatible synthetic polymers (HPMA,*N*-(2-hydroxypropyl)methacrylamide polymers). The results with HPMA polymers were consistent with findings with plasma proteins including, albumin, transferrin and immunoglobulin (6-8).

Lymphotropic characteristics and antimetastatic activity of nanomedicines

We investigated the tissue distribution of a small antitumor protein (NCS,12 kDa) *in vivo* and obtained a fascinating result: when we injected NCS subcutaneously, we found a marked accumulation in regional lymph nodes (1,9-11). This finding prompted us to make NCS more lymphotropic by conjugating it with a hydrophobic polymer, styrene-co-maleic acid (SMA) polymer, to produce SMANCS. That is, we synthesized SMANCS, which accumulated in lymph nodes more than any other tissues (10).

Lymphatic metastasis is the most formidable problem in cancer treatment, but metastatic tumors, which may be seen as small tumor nodules with diameters less than 0.5 mm, do in fact exhibit the EPR effect (12). One of the advantage of lymphotropism of

4

such polymeric conjugates (SMANCS) was therefore effectiveness against lymphatic

metastasis (1,6,10-12). It should be noted that metastatic tumor nodules are fed by

blood vessels (neovasculature), not by the lymphatic system as they grow (13).

The power of the lipid formulation

SMANCS, unique in its high lipophilicity, has styrene residues that make oily

formulations possible by using lipidic X-ray contrast agent [Lipiodol®]. SMANCS in

Lipiodol® can be administered via tumor-feeding arteries, such as the hepatic artery for

hepatoma, and can accomplish the highest effective tumor-selective targeting of drugs

[tumor/blood ratio > 1000 (14)]. SMANCS in Lipiodol® yielded the most impressive

regression of hepatomas, renal cell carcinomas, gallbladder and pancreatic cancers,

and metastatic liver cancers (15,16). This Lipiodol® formulation has at least two

advantages: it yields a clear tumor image by CT-scan (6,14-16), and one can obtain

semiquantitative data about the amount of drug retained in tumors as white area in

tumor.

Another advantage of the oily formulation was that oral delivery of peptide- and

protein- derivatives became possible, because this formulation was stable in gastric

juice and improved absorbability from the intestine more than 17-fold compared with the